NHTSA's REVIEW OF HIGH-RESOLUTION LOAD CELL WALLS' ROLE IN DESIGNING FOR COMPATIBILITY

Matthew B. Jerinsky
William T. Hollowell
National Highway Traffic Safety Administration
USA
Paper #393

ABSTRACT

With the increasing ratio of light trucks to automobiles in the U.S. fleet over the last decade, vehicle compatibility has come into question. A number of tests and performance criteria are under development worldwide to quantify a vehicle's structural design in frontal impacts. These tests and criteria record the force exerted by a vehicle structure onto a high-resolution rigid wall to determine the height from ground of the average force as well as its gradient across the load cells. This paper presents NHTSA's computer simulation research of these vehicle performance tests as they pertain to vehicle compatibility. A number of frontal impact scenarios of a light truck impacting various load cell walls with and without a deformable face are simulated. Changes are made to the vehicle's structure, and the effects to the evaluation criteria are presented.

INTRODUCTION

There are numerous front impact performance tests used by government, media, and industry that measure a vehicle's ability to protect its occupants in a crash with a vehicle within its weight class. These tests are useful in understanding a vehicle's performance within a specific class, but the tests do not address the vehicle's aggressivity [1] or vulnerability in a crash with a vehicle from a different class.

Worldwide research is ongoing to quantify a vehicle's structure through performance test and criteria to ensure the aggressivity/vulnerability balance across vehicle classes [2,3]. This is addressed as a vehicle's compatibility, which is predominately associated with a vehicle's mass, structural interaction, and stiffness [4].

One major development is the addition of high-resolution load cell walls to present performance tests. The load cell walls (LCW) are either rigid or rigid faced with deformable honeycomb sections of various strengths and depths [5,6]. Also, the barriers can be moving or stationary.

NHTSA is researching and developing these various barrier designs for use in performance testing. The research encompasses physical testing [7] as well as computer simulation. This paper summarizes the computer simulation research plan used to review the high-resolution load cell wall and performance criteria as a tool to quantify a vehicle's compatibility.

PROJECT SCOPE

Physical testing of all the various designs for compatibility performance tests is cost prohibitive, so a simulation plan has been developed at NHTSA to aid in the design of compatibility performance tests and criteria. This plan is shown in Figure 1.

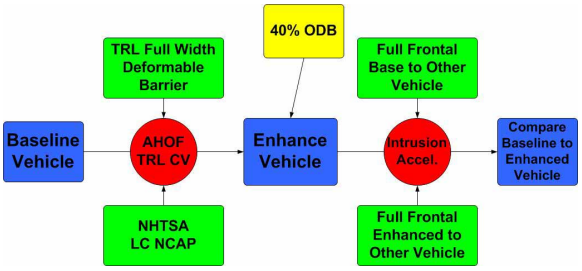

Figure 1. NHTSA's Simulation Plan for High-Resolution Load Cell Wall Review.

The plan can be viewed as two parts. First the full-scale vehicle model will be simulated and validated under US New Car Assessment Program (NCAP) conditions, which are 56 kph, full width overlap, and rigid wall. Simulations will be repeated using three LCW designs. The focus will be to select one of the three LCW designs by using two potential performance criteria as the guide, the Average Height of Force (AHOF) and the Coefficient of Variation (CV). Changes will then be applied to the vehicle models to enhance their respective performance criteria measurements. Since the focus is on the load cell walls and the performance criteria, the changes are not meant for design direction but for testing the robustness of the LCWs and the criteria.

Second, the modified vehicle models will be simulated in vehicle-to-vehicle full frontal test

conditions with both vehicles traveling at 56 kph. Vehicle intrusion and acceleration will be recorded for comparison. These simulations will show the effects of the design changes that were led by the performance criteria.

As a check of self-protection, the fixed 40% offset deformable barrier frontal impact at 64 kph is simulated, and intrusion and acceleration are compared.

Models and Analysis

Barriers

Three barriers are under review. The first is the 2108.2 mm x 984.25 mm, US NCAP, 4x9 load cell wall [8]. The second is a 2000 mm x 1000 mm high-resolution load cell wall built from 125mm x 125mm load cells in an 8x16 matrix. The LCWs are overlaid in Figure 2.

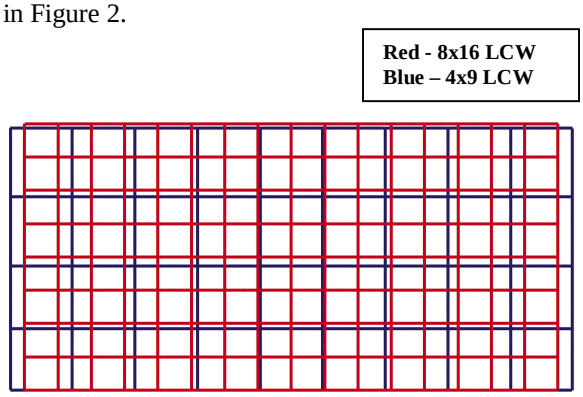

Figure 2. 4x9 NCAP LCW Overlaying 8x16 LCW.

The third wall is under development at the Transport Research Laboratory in the UK [5]. It is a full width 2000 mm x 1000 mm, deformable LCW with an 8 x 16 matrix of 125 mm square load cells. It is faced with a 150 mm layer of 0.34 MPa honeycomb, and a 150 mm slotted layer of 1.71 MPa honeycomb. The 300 mm of honeycomb depth and orientation is shown in Figure 3.

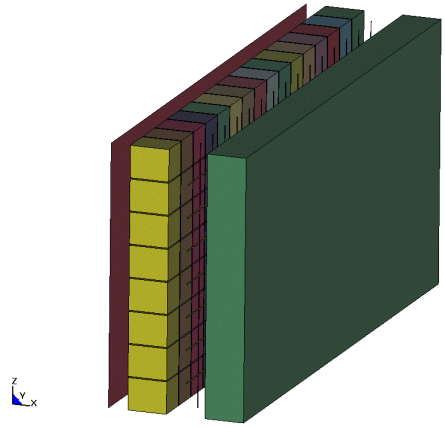

Figure 3. TRL300 8x16 LCW.

Performance Criteria

Two performance criteria are under review: Average Height of Force and TRL's Coefficient of Variation [5]. NHTSA is developing the AHOF calculation to measure the average height of force that a vehicle imparts on a LCW [9]. The intent is to promote structure interaction between vehicles by aligning their stiffest members in the vertical direction. This calculation is shown in Figure 4.

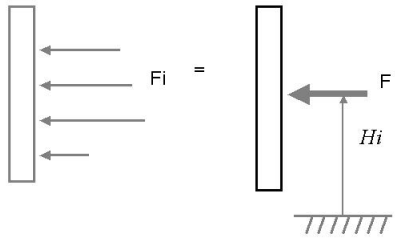

$$\text{AHOF} = \frac{\sum_{1}^{N} FiHi}{\sum^{N} Fi} \qquad (1.)$$

Figure 4. Calculation of AHOF.

The second criterion, TRL's CV [5], measures a vehicle's force homogeneity across its footprint on a load cell wall.

CV = Standard Deviation/Mean (2.)

The standard deviation is calculated at each time point and is a measure of how widely the measured force values are dispersed from the average force value on the LCW. The standard deviation is then divided by the mean value at each time point in order to give the Coefficient of Variation.

Vehicles

NHTSA has developed a number of full-scale frontal impact vehicle models through reverse engineering production vehicles. These models are in various states of development following the continuous improvements being made to techniques in reverse engineering. The two models used in this study are the 1997 Ford Explorer developed by Oak Ridge National Laboratory, and the 1997 Geo Metro developed by the National Crash Analysis Center. The Explorer and Metro are illustrated in Figures 5 and 6, respectively. These models were selected since they are the best examples in the NHTSA model database to represent the compatibility issue of a SUV impacting a small car. Since modifications were made to each model outside the scope of the production vehicle, the Explorer is referred to as "SUV" while the Metro is referred to as "Small Car" for the purposes of this paper. In the future more vehicle classes will be added to the simulation matrix.

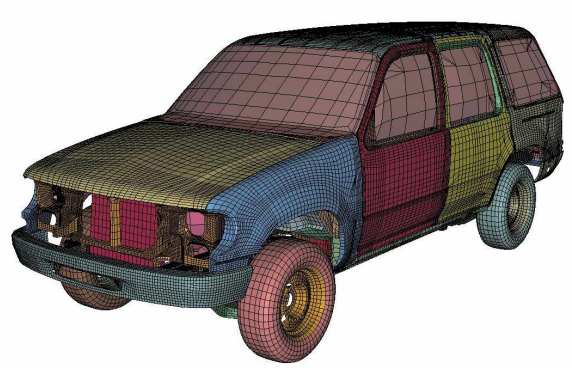

Figure 5. Mid-Size SUV, 1997 Ford Explorer.

Figure 6. Small Car, 1996 Geo Metro.

RESULTS

Full Frontal Impact Mid-Size SUV

The baseline and design iterations of the SUV were simulated in a matrix of three LCW design conditions. For iteration 1 the rails and engine were lowered 50 mm since popular SUVs advertise such changes in new vehicles as a way to increase compatibility [7,10]. The AHOF for each simulated condition is summarized in Table 1.

Table 1. Mid-Size SUV NCAP AHOF

	4x9 NCAP LCW	8x16 NCAP LCW	8x16 TRL300 LCW
Baseline	695 mm	659 mm	658 mm
Iteration1	634 mm	614 mm	608 mm

Comparing the 4x9 to the 8x16 LCW it can be surmised that the AHOF calculation is dependent on the size of the load cells. Figures 7 and 8 present the alignment of the rails and engine to the load cells. The rails, which are in yellow, are aligned with a higher row of load cells in the 4x9 LCW case. The 8x16 LCW splits the same load between two rows of load cells, which results in recording the force at a lower row. This results in a higher AHOF for the 4x9 LCW, and a lower AHOF for the 8x16 LCW.

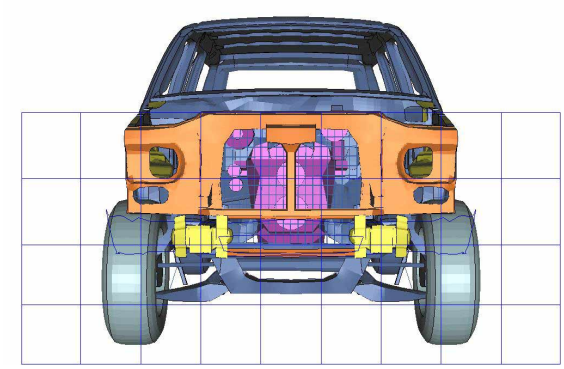

Figure 7. Mid-Size SUV with 4x9 LCW.

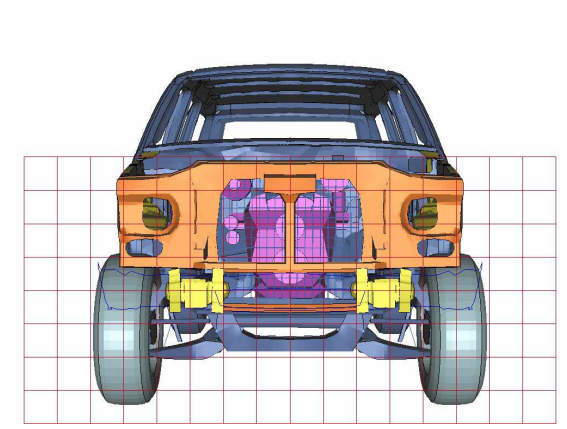

Figure 8. Mid-Size SUV with 8x16 NCAP LCW.

Also from the AHOF measurements one can see that the deformable face in the TRL300 LCW does not appreciably change the AHOF results even though the total wall force is quite different as seen in Figure 9. As expected, the 4x9 and 8x16 LCW show the same total measured force.

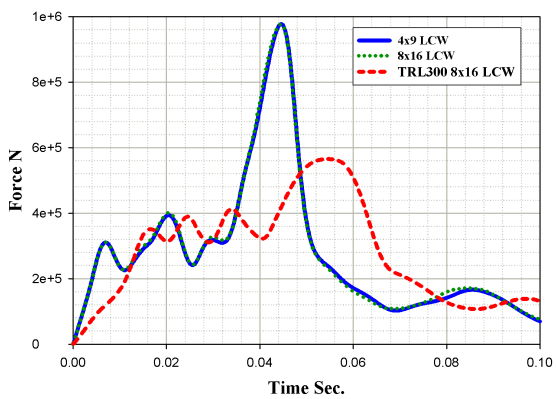

Figure 9. Mid-Size SUV LCW Total Force.

Baseline

Contour plots of the force applied to the LCW are a good visual tool to review which structural members of the vehicle apply the load. The contour plots presented in this paper are created from point loads centered at each load cell and then averaged between these point loads. For this reason the accuracy of the area reflected in the contour plot by the force loading is reduced with coarser LCWs. Also, the scale for the force will change based on the point loads and not the surface area covered by each load cell.

From Figure 9 the LCW force curve can be broken into two parts, the initial force loading of the structure and the maximum total force. This is at 20 msec. and 45 msec. for the 4x9 and 8x16 LCWs, and at 34 msec. and 56 msec. for the TRL300 LCW.

The 4x9 and 8x16 LCWs without honeycomb are shown in Figures 10 and 11. At 20 msec. the rails have hit the wall and are crushing. The rails are the dominant structural members at this time. Since the rails hit the edge of a higher load cell in the 4x9 case, the contour plot shows how the load is spread to higher load cells than the 8x16 LCW.

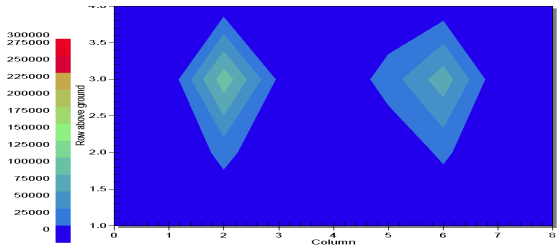

Figure 10. SUV 4x9 NCAP LCW Contour at 20 msec.

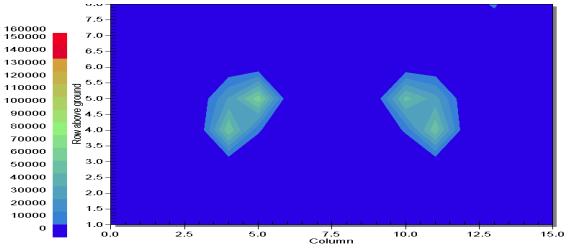

Figure 11. SUV 8x16 LCW Contour at 20 msec.

At 45 msec., which can be seen in Figures 12 and 13, the engine and vehicle stack into the wall, and the load is again spread into higher load cells in the 4x9 LCW case. Since the load is concentrated, the 8x16 LCW can better separate the dominant members from lesser load path contributors. This will help in promoting homogeneity to a vehicle's front structural stiffness by reducing the concentrated loads through a performance criterion such as CV. The 8x16 LCW is a good first step, but further research is needed to find the best compromise between load cell size and cost.

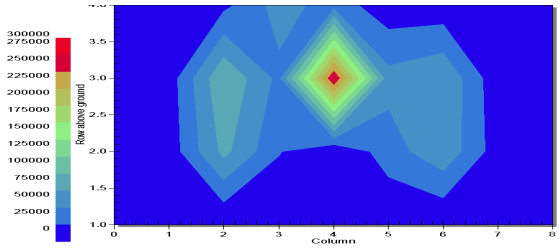

Figure 12. SUV 4x9 NCAP LCW Contour at 45 msec.

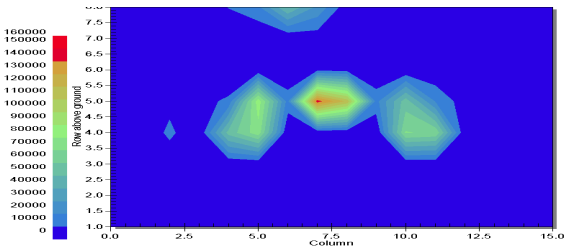

Figure 13. SUV 8x16 LCW Contour at 45 msec.

The TRL300 LCW separates the load paths even further. This is shown in Figures 14 and 15. The engine does not stack up against the wall as severely as measured by the LCW in Figure 9. Instead, the loads from the rails are measured for the duration of the crash. This would be useful in measuring vehicle load paths such as cross members, sub-frames, and shotguns, which would be overshadowed by the engine stack up. However, more research is needed to select the honeycomb properties since these load paths are not readily shown in the present contours.

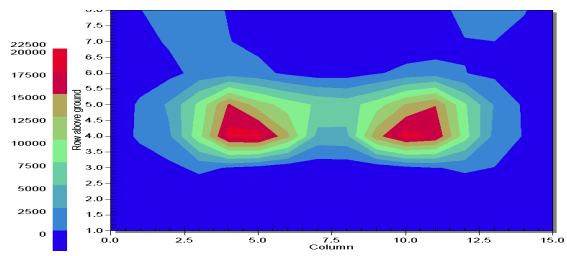

Figure 14. SUV 8x16 TRL300 LCW Contour at 34 msec.

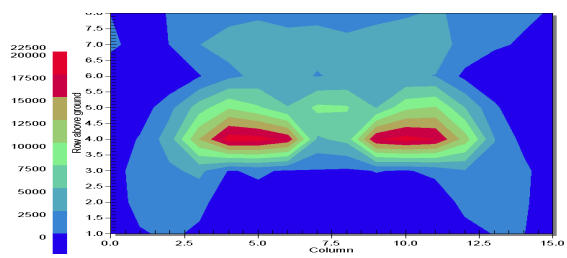

Figure 15. SUV 8x16 TRL300 LCW Contour at 56 msec.

The CV values for each case are plotted in Figure 16. The CV values for the TRL300 LCW are lower with less fluctuation. This confirms the less severe impact of the engine and the difference in force between the front structure and the engine. Also, iteration 1 for the 8 x 16 LCW has a higher CV initially than the baseline. This may be caused by the force loading from the rails being split between two load cells rather than four as in the baseline. This needs more investigation with CV.

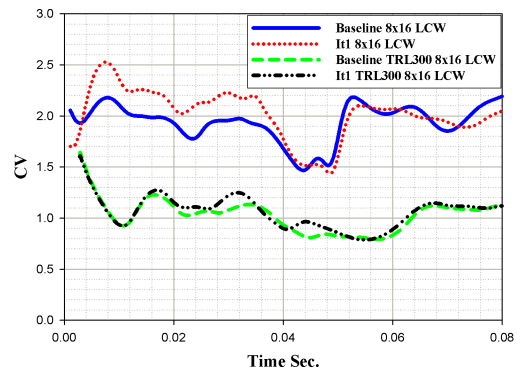

Figure 16. Mid-Size SUV LCW CV

The honeycomb displacement contours at 35 and 55 msec. are shown in Figures 17 and 18. These two times show the deformed honeycomb at the peak of the rail crush, and the onset of the engine stack up. From the deformed geometry it is evidenced that the shotguns, hood and wheels are potential load paths that can be measured dependent on the LCW resolution and honeycomb properties. However, care must be taken to not distort the actual stiffness of the vehicle structure.

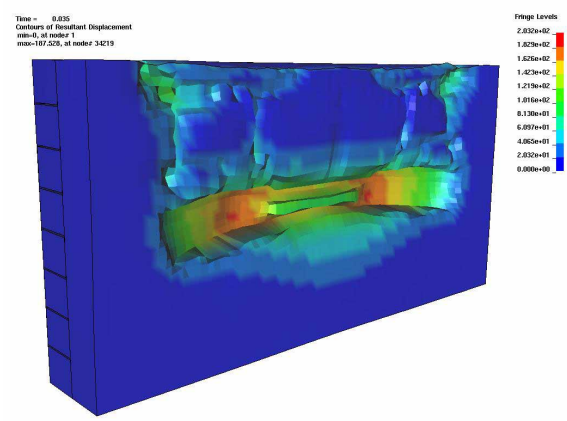

Figure 17. SUV 8x16 TRL300 Honeycomb Displacement Contour at 35 msec.

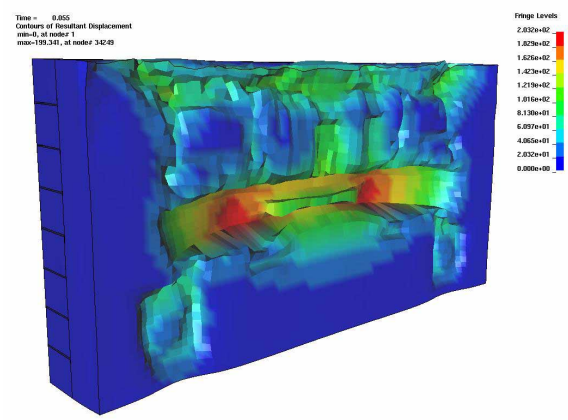

Figure 18. SUV 8x16 TRL300 Honeycomb Displacement Contour at 55 msec.

Iteration 1

In an attempt to promote structural interaction between the Small Car and the SUV, the rail and the engine of the SUV model were lowered 50 mm, while the rest of the vehicle was maintained at baseline conditions. Table 1 lists a 45 mm drop in calculated AHOF for the 8x16 case. This is encouraging since the dominant members in a frontal impact directly control the AHOF, as would be expected.

Figures 19, 20, and 21 illustrate the contours at engine stack up for the respective cases. As in the baseline simulations, it is shown that the 4x9 LCW is less accurate in measuring the AHOF. Additionally, the TRL300 LCW records the bumper and rail load as the peak even through the engine stack up.

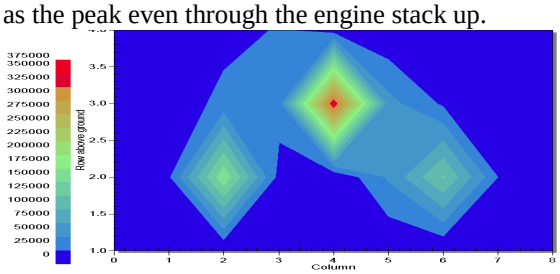

Figure 19. SUV Iteration 1 4x9 NCAP LCW Contour at 45 msec.

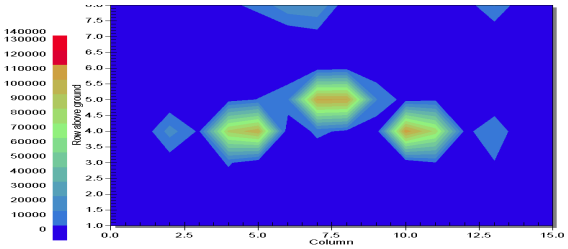

Figure 20. SUV Iteration 1 8x16 LCW Contour at 45 msec.

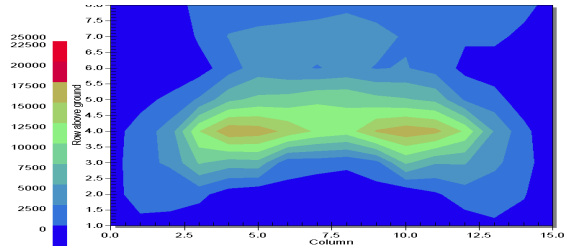

Figure 21. SUV Iteration 1 8x16 TRL300 LCW Contour at 56 msec.

In Figure 22 the lowered distance of the rails and bumper can quickly be seen when compared to Figure 18. For this study, using the CV to initiate design was not addressed. In future iterations specific changes to the structure will be made to enhance the vehicle's CV, and the effects will be reviewed in vehicle-to vehicle crash conditions. Also, a more complete investigation into CV will be presented.

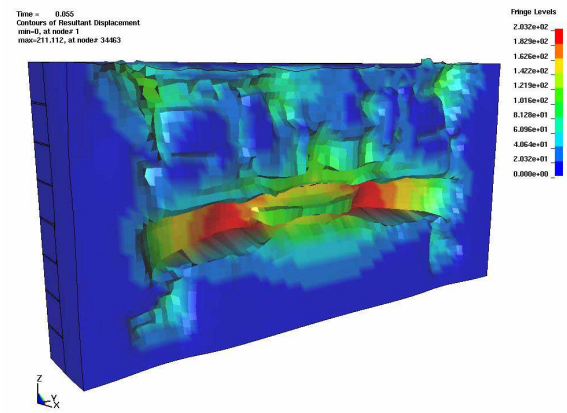

Figure 22. SUV Iteration 1 8x16 TRL300 Honeycomb Displacement Contour at 55 msec.

Full Frontal Impact Small Car

The simulation test plan is also applied to the small car to possibly harmonize the AHOF for the two vehicles. The AHOF results are summarized in Table 2. Iteration 1 is simply the entire vehicle moved upward 25 mm since this is achievable in real world vehicles through suspension changes. For this reason, the results of iteration 1 are summarized and no detailed contours are provided since they are not significantly different than the baseline.

Table 2. Small Car NCAP AHOF

	4x9 NCAP LCW	8x16 LCW	8x16 TRL300 LCW
Baseline	525 mm	525 mm	495 mm
Iteration1	540 mm	538 mm	510 mm

In the Small Car case the effects of load cell resolution is not seen for AHOF. Figures 23 and 24 show that the rails and bumper are aligned with the same load cell height. Since the rails and bumper are aligned with the same load cell height, the 4x9 LCW and the 8x16 LCW have good correlation.

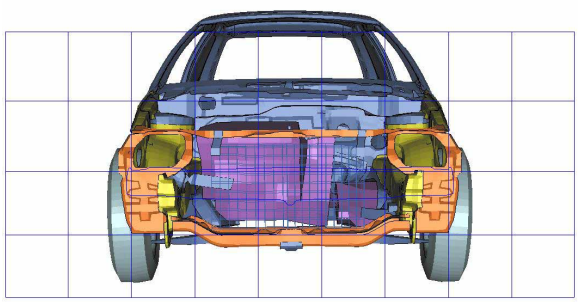

Figure 23. Small Car with 4x9 NCAP LCW.

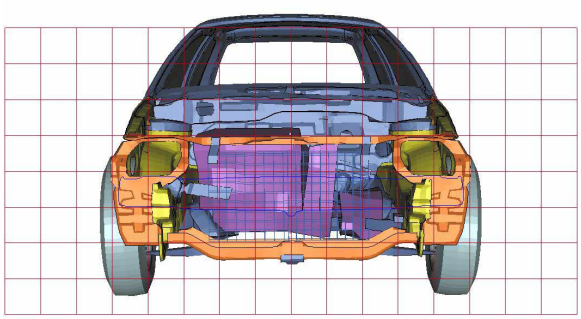

Figure 24. Small Car with 8x16 LCW.

The total forces measured by the LCWs are plotted in Figure 25. The first layer of the TRL300 honeycomb in the Small Car case is stiff in relation to the vehicle's structure and mass, which causes less of a drop in the maximum peak when compared to the SUV.

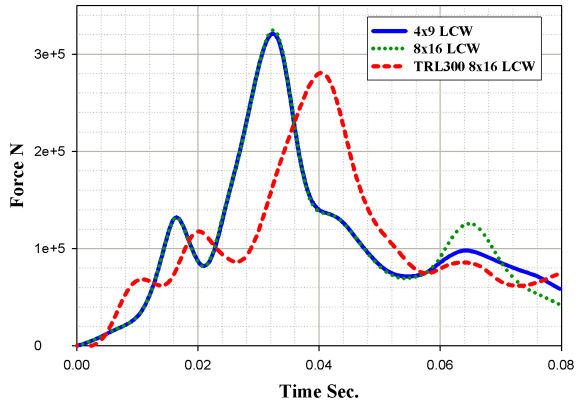

Figure 25. Small Car LCW Total Wall Force

<u>Baseline</u>

Since the Small Car is lighter and unibody, it does not have the same stiffness in longitudinal members when compared to the SUV, but the rails still dominate the front structure as seen in Figures 26 and 27 at early time.

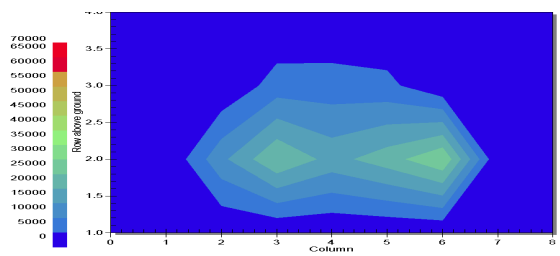

Figure 26. Small Car 4x9 NCAP LCW Contour at 16 msec.

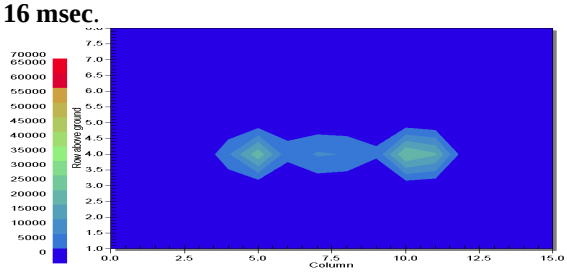

Figure 27. Small Car 8x16 LCW Contour at 16 msec.

However, as the engine and vehicle stack up, the load path is not clear for the 4x9 LCW, which can be seen in Figure 28. The rail loads are comparable to the rest of the vehicle, and the cross members distort the contour since there are half the number of load cells between the rails. The 8x16 LCW, as shown in Figure 29 does not exhibit this issue. The additional load cells across the columns provide more data points to separate the load paths.

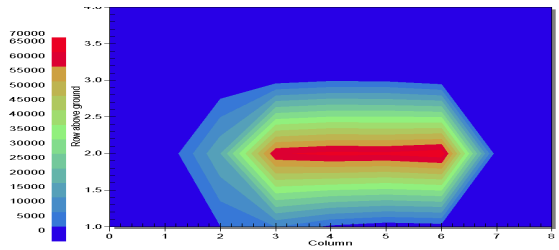

Figure 28. Small Car 4x9 NCAP LCW Contour at 32 msec.

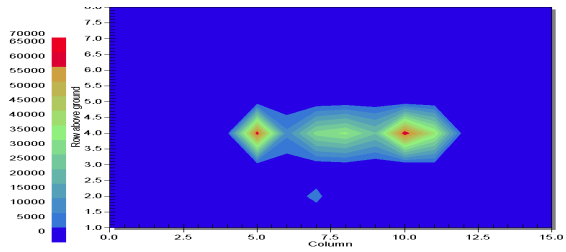

Figure 29. Small Car 8x16 LCW Contour at 32 msec.

The early loads on the wall are measured quite differently in the case of the TRL300 LCW. Figure 30 shows a distribution of load from the rails and the bumper.

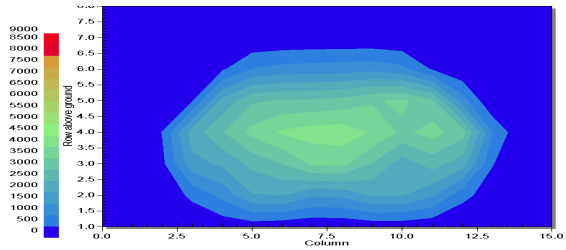

Figure 30. Small Car 8x16 TRL300 LCW Contour at 20 msec.

Also, the TRL300 LCW separates the dominant and lesser load paths at engine stack up in the Small Car simulations. Figure 31 shows how the engine sub-frame is recorded. This is directly shown by the AHOF since the value is 30 mm lower than with the rigid LCW.

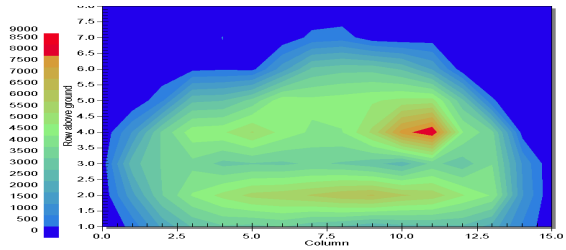

Figure 31. Small Car 8x16 TRL300 LCW Contour at 40 msec.

As shown in Figure 32 the Small Car follows the CV trend found in the SUV case. The values are lower and fluctuate less with the TRL300 LCW. The stiffness differential between the rails and engine mass is greater for the Small Car since it is lighter with weaker rails when compared to the SUV. This creates a larger fluctuation in the CV calculation. Future iteration studies will be made to lower these fluctuations in order to understand CV effects.

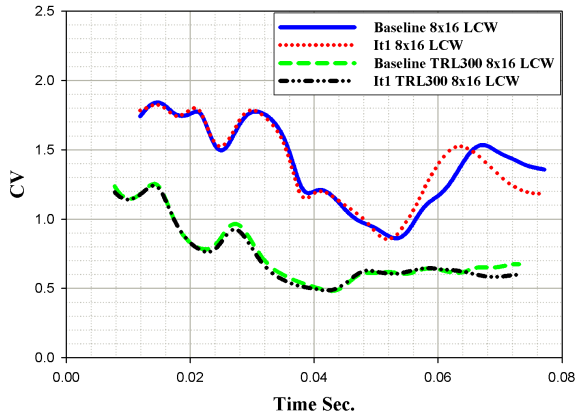

Figure 32. Small Car LCW CV.

When compared to the SUV, the deformed honeycomb for the Small Car shows less compression outside the areas of the bumper beam. Figure 33 depicts the deformed honeycomb at 20 msec., which is caused by the front structure before crush is complete.

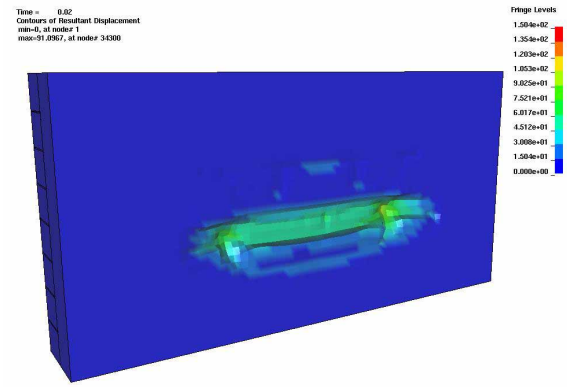

Figure 33. Small Car 8x16 TRL300 Honeycomb Displacement Contour at 20 msec.

In Figure 34 the shotgun and lower cross member compression on the honeycomb can be seen.

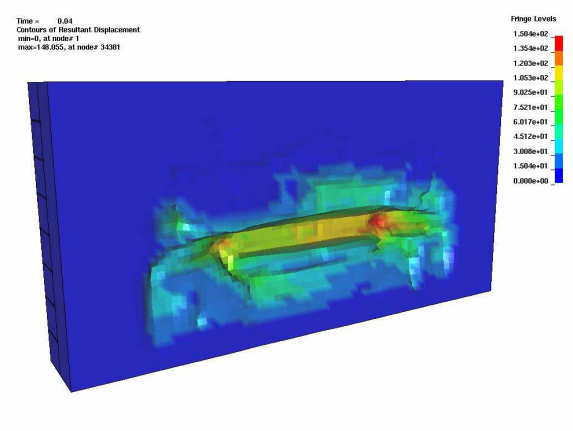

Figure 34. Small Car 8x16 TRL300 Honeycomb Displacement Contour at 40 msec.

Observations of AHOF and TRL300

The TRL300 LCW influences the calculated AHOF for the Small Car, but not the SUV. A closer review of AHOF and the TRL300 LCW can explain this.

Since the AHOF weights the calculation based on the time window of the highest loading, the AHOF calculated before engine stack up is not easily seen. Tables 3 and 4 list the calculated AHOF of the Small Car and the SUV's first set of force peaks or initial AHOF. These force peaks, as seen from the contour plots, are related to the structural loading before the engine stacks into the wall. The total AHOF from Tables 1 and 2 is included for comparison.

Table 3. Small Car Initial & Total NCAP AHOF

	Small Car AHOF mm			
	Initial	**Total**	**Initial**	**Total**
	8x16 LCW	*8x16 LCW*	*8x16 TRL300 LCW*	*8x16 TRL300 LCW*
Baseline	505	525	460	495
Iteration1	518	538	484	510

Table 4. SUV Initial & Total NCAP AHOF

	SUV AHOF mm			
	Initial	**Total**	**Initial**	**Total**
	8x16 LCW	*8x16 LCW*	*8x16 TRL300 LCW*	*8x16 TRL300 LCW*
Baseline	613	659	614	658
Iteration1	568	614	564	608

In the case of the Small Car, the initial AHOF for the rigid LCW when compared to the total AHOF for the TRL300 LCW shows little difference. In this situation the honeycomb properties are helpful. The honeycomb works as designed where the first layer bottoms out separating the structure from the engine, while the stiffer second layer maintains load transfer to the LCW. This can be seen in Figure 35.

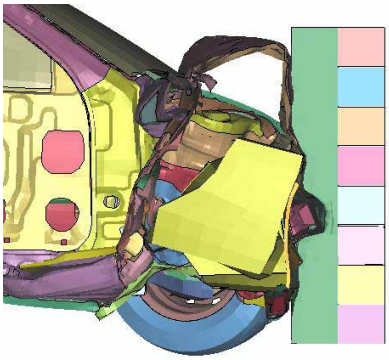

Figure 35. Small Car 8x16 TRL300 Honeycomb Deformed Cross Section.

The opposite is true for the SUV. Figure 36 illustrates the issue for the SUV case. The second layer is compressed and the vehicle loads the LCW through the stiffened honeycomb elements. This causes the calculated AHOF for the TRL300 LCW to match the rigid LCW values. Therefore, the TRL300 LCW is questionable for use across the US vehicle fleet and needs further research.

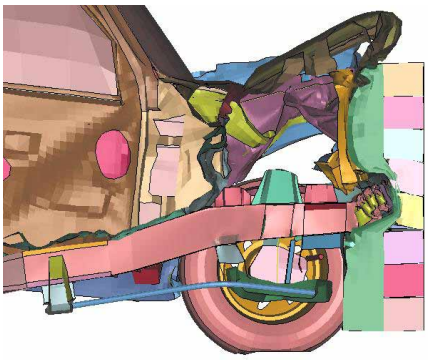

Figure 36. SUV 8x16 TRL300 Honeycomb

In this study the selection of the TRL300 honeycomb properties are biased to the Small Car and in the future should be chosen to limit bias to a particular vehicle class. Since the Explorer is a mid-size SUV, this issue will be more important for a large SUV or van, which may overpower the TRL300 honeycomb

negating the intent of separating the load paths from engine influences.

Offset Deformable Barrier Impact (ODB)

<u>Mid-Size SUV</u>

The offset deformable frontal test measures the vehicle structure performance as well as the dummy. This intrusion needs to be maintained to ensure vehicle vulnerability changes are kept to a minimum. For this reason the SUV was simulated in the ODB test condition.

Figure 37 shows similar acceleration results in the occupant compartment while Figure 38 shows the intrusion results. The occupant compartment experiences the same acceleration, but the intrusion increases for iteration 1.

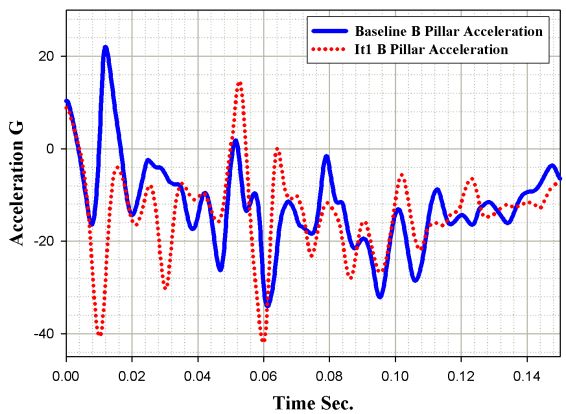

Figure 37. Mid-Size SUV Frontal, 40% ODB B Pillar Acceleration.

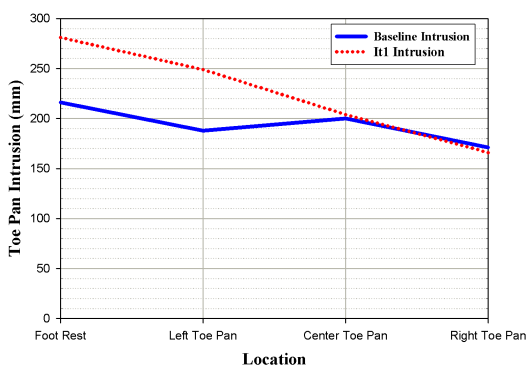

Figure 38. Mid-Size SUV Frontal, 40% ODB Toe Pan Intrusion.

This is caused since the rail has a different crush mode from baseline. The Body-In-White (BIW) mounting distance from the frame is higher for iteration 1, so a larger moment is created on the rail, which bends at the frame mount under the left footrest. This drives the rail into the occupant compartment. In future runs this torque will be minimized to lessen the effects to the ODB performance.

Vehicle-to-Vehicle Impact

The final review of the LCWs and the performance criteria effects is completed in vehicle-to-vehicle test conditions. Each vehicle is given a 56 kph initial velocity and impacted with full overlap conditions. The matrix is listed in Table 5.

Table 5. VTV Iteration Summary

	Vehicle	
	Mid-Size SUV	**Small Car**
Baseline	*Baseline SUV*	*Baseline Small Car*
Iteration 1	*SUV with 50mm drop in rails and engine.*	*Baseline Small Car*
Iteration 2	*SUV with 50mm drop in rails and engine.*	*Small Car raised 25mm.*

The three cases are depicted in Figures 39, 40, and 41. The iterations increasingly align the vertical heights of the rails, which correlate with the AHOF measured, as previously shown in Tables 3 and 4.

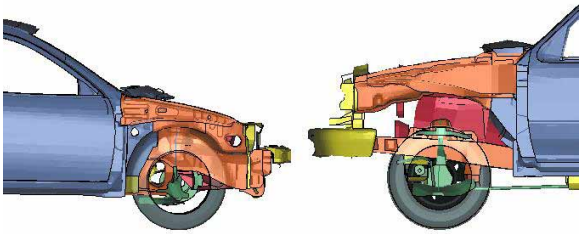

Figure 39. Pre-crash Baseline - SUV to Small Car Side View.

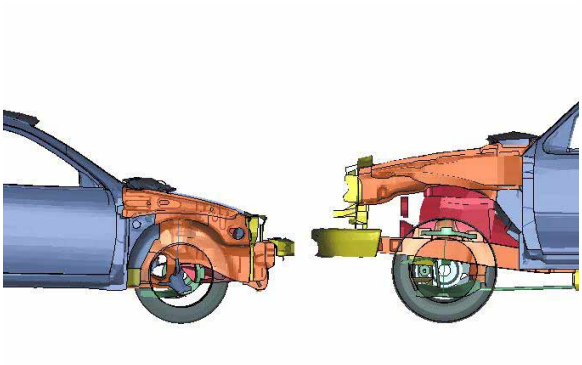

Figure 40. Pre-crash Iteration 1 - SUV to Small Car Side View.

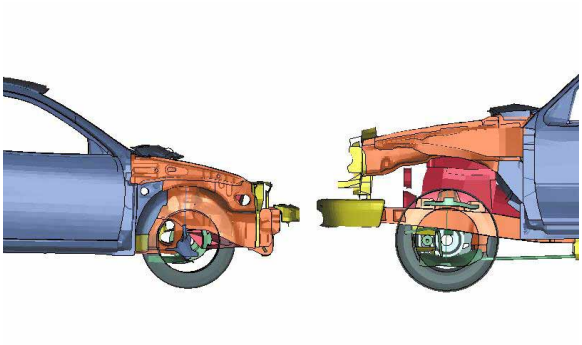

Figure 41. Pre-crash Iteration 2 - SUV to Small Car Side View.

Figure 42 illustrates the deformed vehicles at maximum displacement for baseline conditions. The SUV overrides the Small Car with little interaction of the rails, and no interaction with the engine, which are the two peak load paths shown in the LCW study. The subsequent iterations are simulated in an attempt to increase the structural interaction by using the combination of vehicles that reduce the AHOF value.

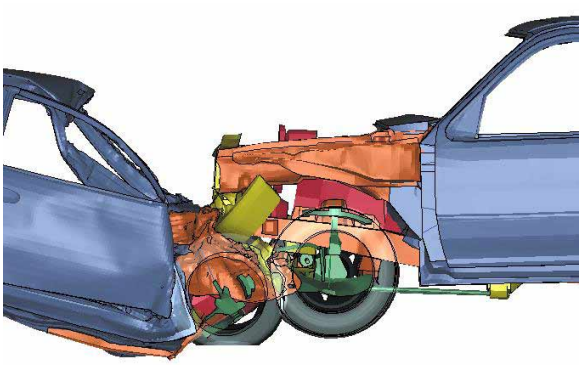

Figure 42. Baseline - SUV to Small Car Maximum Deformation Side View.

Since the models are not advanced enough to include the dummy models, intrusion measurements and the occupant compartment accelerations are summarized as the main criteria to compare the three cases. In the future, dummy models will be included in an attempt to capture occupant injury values.

Small Car Intrusion

The Small Car intrusion measurements were recorded at the locations viewed in Figure 43.

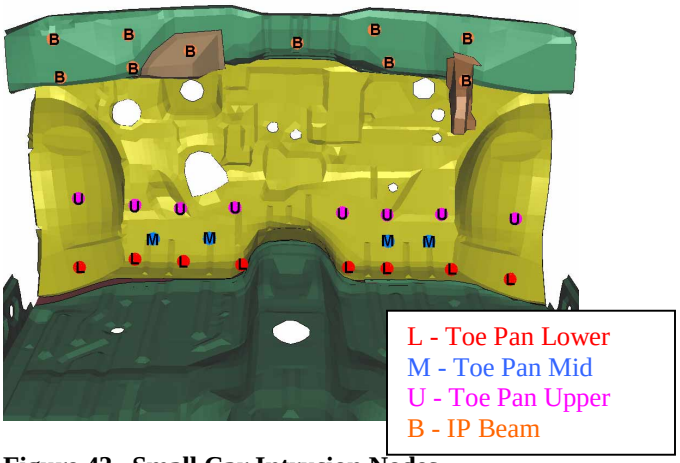

Figure 43. Small Car Intrusion Nodes.

Each measurement was compared, and the maximum intrusions measured are plotted in Figures 44 to 48. In most locations iteration 1 has lower intrusion than baseline. In iteration 2 the intrusion is either the same as the baseline or higher except at the instrument panel (IP) beam. This may be caused by the lower capacity of the Small Car's bumper and rail joint in axial crush when compared to the SUV. Further simulation iterations need to be reviewed to answer this.

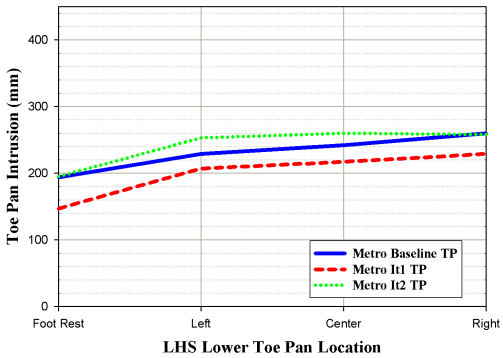

Figure 44. Small Car LHS Lower Toe Pan Intrusion.

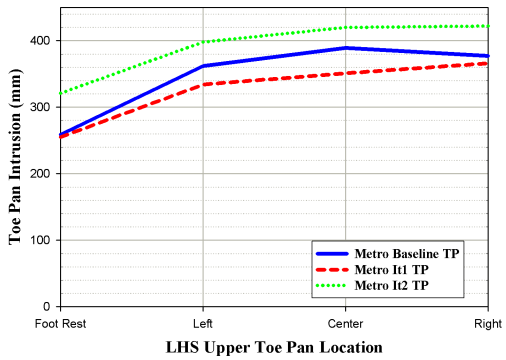

Figure 45. Small Car LHS Upper Toe Pan Intrusion.

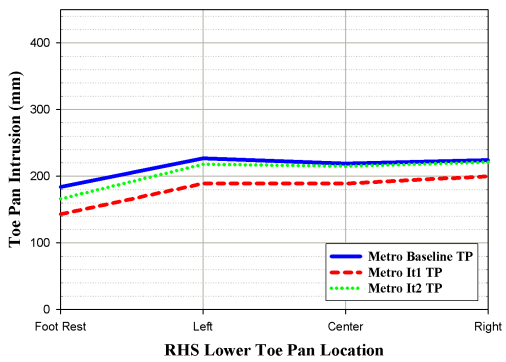

Figure 46. Small Car RHS Lower Toe Pan Intrusion.

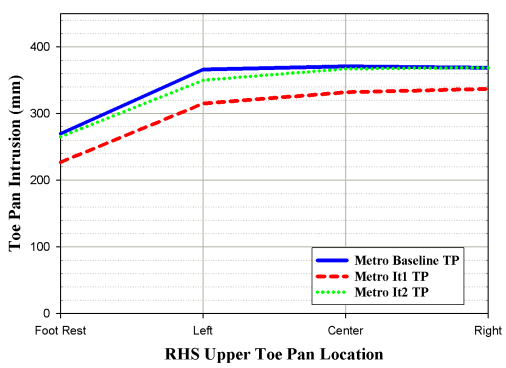

Figure 47. Small Car RHS Upper Toe Pan Intrusion.

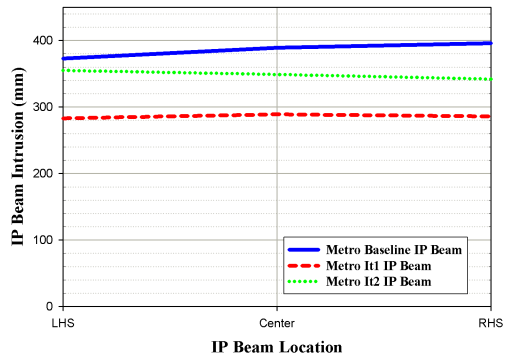

Figure 48. Small Car IP Beam Intrusion.

Since override is reduced in iteration 1 and 2, less intrusion into the IP beam is expected and is seen. The toe pan decreases as well for iteration 1. This may be caused by more energy absorption of the SUV.

Mid-Size SUV Intrusion

The SUV model's intrusion is measured at the same location as in the ODB test. The results are graphed in Figure 49. Iteration 1 points to better structural interaction as with the Small Car since the intrusion is increased when compared to baseline and iteration 2. Iteration 2 has only one point with better intrusion numbers. This confirms the additional interaction between the rails leads to the SUV sharing in the energy absorption decreasing the intrusion measured in the Small Car.

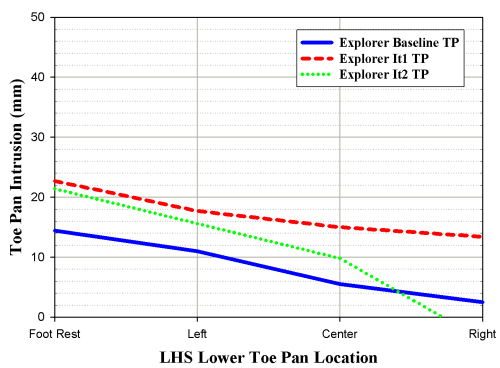

Figure 49. SUV Toe Pan Intrusion.

Deformed Cross Sections

Review of the deformed plots and cross sections of the two vehicles show better structural interaction for

iteration 1 when compared to baseline or iteration 2. This can be seen in Figures 50, 51, and 52.

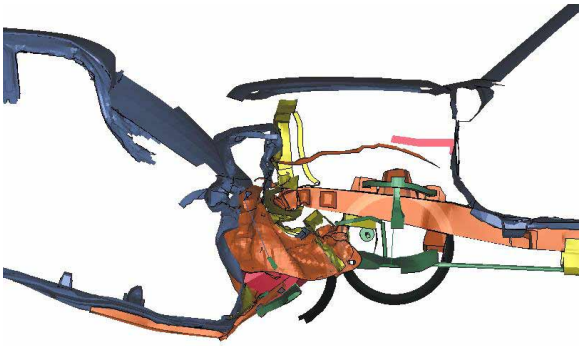

Figure 50. Baseline - SUV to Small Car Maximum Deformation LHS Section View.

In Figure 51 the crush of the rails is noticeable as none of the crush initiators, which are located on the rail forward of the engine, are visible. This is not the case for the baseline and iteration 2.

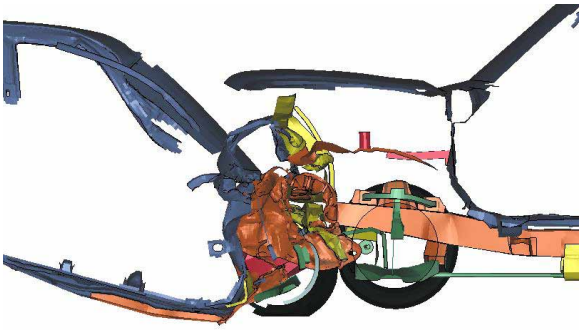

Figure 51. Iteration 1 - SUV to Small Car Maximum Deformation LHS Section View.

Iteration 2 shows more bending than crush in Figure 52. This would place more of the energy absorption to the Small Car, which is recorded in the intrusion numbers.

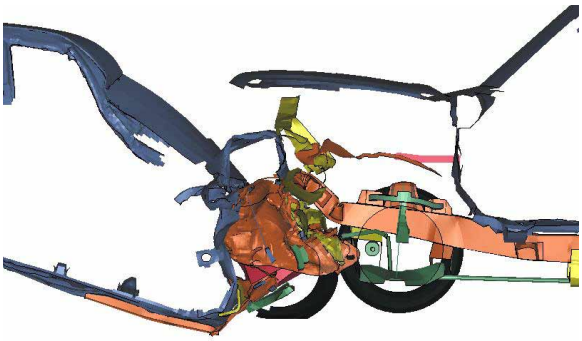

Figure 52. Iteration 2 - SUV to Small Car Maximum Deformation LHS Section View.

Depending on which AHOF measurement is used, the difference in AHOF between the vehicles for iteration 2 can vary from as little as 10 mm to as much as 30 mm. Since the rails are not fully crushed, in any of the cases, the SUV's engine does not load into the Small Car. Iteration 2 shows that structural interaction is the first step, but since the SUV's rails are not fully crushed, the stiffness of the vehicle should also be used to optimize for compatibility. AHOF coupled with an upper and lower bound for vehicle force may be needed to reduce this issue since the Small Car cannot maintain the occupant compartment. Further research into vehicle structural stiffness is needed to answer this issue.

Small Car Velocity and Acceleration

Lastly, the Small Car's occupant compartment acceleration is shown in Figure 53. Each case is on the same order of magnitude, and the timing is comparable. However, the first spike in iteration 1 is inverted and lower when compared to the baseline and iteration 2. This may be caused by the increase in structural interaction. As the Small Car impacts the SUV, the rails are better utilized allowing the vehicle to slow by being pushed backwards. At the same time, the rails are crushing and absorbing energy. Further investigation with iterations including the dummy models is needed to fully understand the effects on injury criteria.

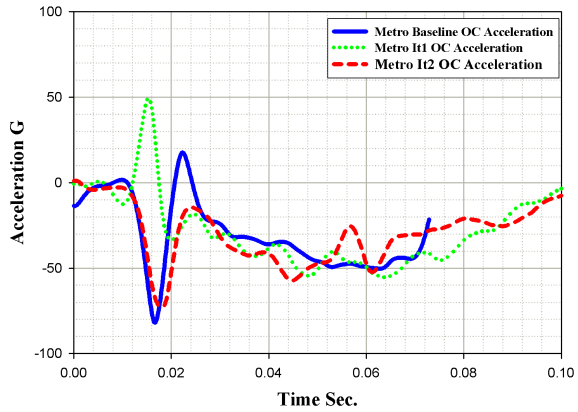

Figure 53. Small Car Occupant Compartment Acceleration.

FUTURE WORK

The work presented in this paper has shown the first step NHTSA is making in reviewing high-resolution load cell walls. The next step is to develop parameters from vehicles of different classes to study. Each parameter such as mass, initial stiffness,

and speed will be varied to study the effects on the performance criteria discussed, and how those effects ultimately change vehicle performance in vehicle-to-vehicle test conditions. Also, a movable deformable LC barrier will be added to the simulation plan. The updated plan is shown in Figure 54.

The plan will be revised as new developments are made in the validity of the performance criteria, or new criteria are introduced.

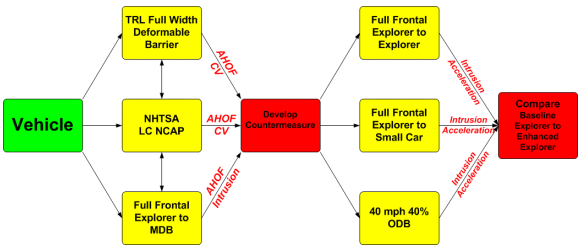

Figure 54. Revised NHTSA Simulation Plan.

Finally, the plan will be worked in reverse. A compatible mid-size SUV and small car will be developed based on the vehicles and results of this paper. Those vehicles will be impacted into the LCWs to find if the performance criteria predict their compatibility weaknesses and strengths as designed.

CONCLUSION

The load cell wall can be an effective tool in measuring and quantifying a vehicle's structure in a frontal crash. Its effectiveness depends on the resolution available, and the performance criteria used.

The AHOF is useful in determining a vehicle's vertical structural interaction across different classes. However its accuracy depends on the resolution of the load cell wall. When the LCW resolution is too coarse and the vehicle's dominant structural load paths bridge the edge of an adjoining load cell, the average will be distorted. AHOF is also dependent on the load cell wall's ability to separate the structural loads from contributors such as the engine. In certain cases the vehicle's engine load on the load cell wall can reduce the effect of the recorded force of the vehicle's structure, which is important for vehicle-to-vehicle crashes where the structure does not always crush into the engine.

TRL's deformable barrier addresses this issue, but care must be taken on correctly choosing the honeycomb stiffness and depth to prevent interfering with the crush mode or load of the structural members. Also, shear between honeycomb blocks must be prevented to ensure accurate longitudinal measurements. In certain cases TRL's deformable barrier also records load from structural cross members, which would be missed if a rigid wall is used. These cross members are also essential for offset crashes and side impact scenarios, and must be measured accurately. Further investigation into TRL's CV may provide the criterion to quantify this.

Compatibility is more than just a vehicle's structural interaction. However, the use of load cell walls, coupled with the performance criteria reviewed in this paper, are a good first step toward addressing compatibility in a frontal crash. Vehicle parameters such as mass and stiffness also play an important role. Additional research is necessary to quantify these parameters through load cell walls and other means.

ADDITIONAL INFORMATION

Additional NHTSA reports on compatibility research are available from http://www-nrd.nhtsa.dot.gov/departments/nrd-11/aggressivity/ag.html

Vehicle models available on the world wide web:

1. 1997 Ford Explorer from ORNL at http://www-explorer.ornl.gov/newexplorer/
2. 1997 Geo Metro from NCAC at http://www.ncac.gwu.edu/archives/model/index.html

REFERENCES

1. Gabler, H.C., Hollowell, W. T., "NHTSA's Vehicle Aggressitivity and Compatibility Research Program", Proceedings of the Sixteenth International Enhanced Safety of Vehicle Conference, Paper No. 98-S3-O-01, Windsor, Canada, 1998
2. Mizuno, K., Tateishi, K., Ezaka, Y., "Test Procedures to Evaluate Vehicle Compatibility", Seventeenth International Technical Conference on the Enhanced Safety of Vehicles, Paper No. 127, Amsterdam, 2001
3. Seyer, K. A., Newland, C.A., Terrell, M.B., "Australian Research to Develop a Vehicle Compatibility Test", Vehicle Safety 2002 Conference, London, May 2002
4. Joksch, H.C., "Vehicle Design versus Aggressivity", University of Michigan Transportation Research Institute, DOT Report HS 809 194, April 2000

5. Edwards, E., Hobbs, A., Davies, H., Thompson, A., "Development of Test Procedures and Performance Criteria to Improve Compatibility in Car Frontal Collisions", Vehicle Safety 2002 Conference, London, May 2002
6. Delannoy, P., Diboine, A., "Structural Front Unit Global Approach", Seventeenth International Technical Conference on the Enhanced Safety of Vehicles, Paper No. 199, June 2001
7. Summers, S., Hollowell, W.T., Prasad, A., "NHTSA'S Research Program for Vehicle Compatibility", Eighteenth International ESV Conference, Paper No. 307, Japan, 2003
8. Summers, S., Prasad, A., Hollowell, W.T., "NHTSA's Compatibility Research Program Update", Society of Automotive Engineers Paper No. 2001-01-1167, March 2001
9. Summers, S., Hollowell, W.T., Prasad, A., "Design Considerations for a Compatibility Test Procedure", Society of Automotive Engineers Paper No. 2002-02B-169, March 2002
10. 2003 Ford Expedition Sales Brochure, page 11, http://www.fordvehicles.com/images/suvs/brochures/EPD03_brochure.pdf